Visualization of Membrane Fusion, One Particle at a Time

ARTICLE *in* BIOCHEMISTRY · FEBRUARY 2013

Impact Factor: 3.02 · DOI: 10.1021/bi301573w · Source: PubMed

2 AUTHORS:

Jason Otterstrom
ICFO Institute of Photonic Sciences
8 PUBLICATIONS **62** CITATIONS
SEE PROFILE

Antoine van Oijen
University of Wollongong
124 PUBLICATIONS **4,364** CITATIONS
SEE PROFILE

BIOCHEMISTRY
including biophysical chemistry & molecular biology

Current Topic

pubs.acs.org/biochemistry

Visualization of Membrane Fusion, One Particle at a Time

Jason Otterstrom[†,‡] and Antoine M. van Oijen*[,‡]

[†]Harvard Biophysics Program, Harvard Medical School, 240 Longwood Avenue, Boston, Massachusetts 02115, United States
[‡]Centre for Synthetic Biology, Zernike Institute for Advanced Materials, Nijenborgh 4, 9747AG Groningen, The Netherlands

ABSTRACT: Protein-mediated fusion between phospholipid bilayers is a fundamental and necessary mechanism for many cellular processes. The short-lived nature of the intermediate states visited during fusion makes it challenging to capture precise kinetic information using classical, ensemble-averaging biophysical techniques. Recently, a number of single-particle fluorescence microscopy-based assays that allow researchers to obtain highly quantitative data about the fusion process by observing individual fusion events in real time have been developed. These assays depend upon changes in the acquired fluorescence signal to provide a direct readout for transitions between the various fusion intermediates. The resulting data yield meaningful and detailed kinetic information about the transitory states en route to productive membrane fusion. In this review, we highlight recent in vitro and in vivo studies of membrane fusion at the single-particle level in the contexts of viral membrane fusion and SNARE-mediated synaptic vesicle fusion. These studies afford insight into mechanisms of coordination between fusion-mediating proteins as well as coordination of the overall fusion process with other cellular processes. The development of single-particle approaches to investigate membrane fusion and their successful application to a number of model systems have resulted in a new experimental paradigm and open up considerable opportunities to extend these methods to other biological processes that involve membrane fusion.

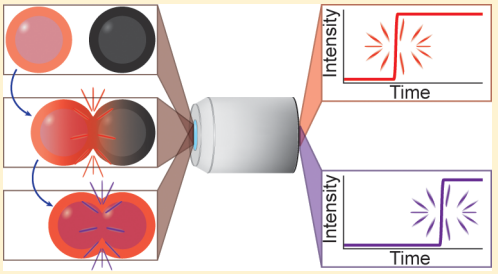

Membranes comprised of phospholipid bilayers are essential for all cellular life. They encapsulate cytoplasmic components, allow for enrichment of metabolites, and restrict the entry of foreign pathogens and damaging chemicals. Further, eukaryotes have developed inner membranes to form organelles that allow for compartmentalization of metabolic and replicative processes. At times, though, this resolute barrier must be perturbed, broken, and subsequently re-formed; namely, membranes must fuse. While the final state of fully merged membranes from two initially separate bilayers is an energetically favorable one, there are many energetic barriers that must be overcome to achieve this final fused state.

Membrane fusion generally occurs through a series of steps, including close bilayer apposition, fusion of the proximal leaflets (termed hemifusion), and finally merger of the distal leaflets (termed pore formation).[1,2] These metastable intermediates along the fusion pathway are depicted in Figure 1 and can be experimentally probed, as will be discussed herein. Significant energetic barriers separating these intermediates make the energetic landscape a rough terrain to traverse. Dehydration of a limited area between two closely apposed bilayers, formed by a fusion dimple or pointlike protrusion, poses the first sizable energy barrier.[2,3] Formation of a hemifusion stalk (Figure 1B) is also energetically expensive, with an energy barrier to formation that can be on the order of ~20−40 k_BT (12−24 kcal/mol, where 1 $k_BT \approx 0.6$ kcal/mol).[1,2,4] The hemifused state can progress in two directions: it can develop into a full fusion pore that allows mixing of the contents initially separated by the two bilayers (Figure 1C), or it can become an extended hemifusion diaphragm that is a kinetic dead end and prevents content mixing.[6] In addition, alternative pathways could supplant the lipidic hemifusion stalk with a nascent proteinaceous pore that subsequently develops into a full lipidic fusion pore.[5,7] Moreover, the initial fusion pore is not necessarily a stable structure, and work is required to drive it open.[5] If a nascent fusion pore is prone to collapse, what is the lifetime of a pore and what pore size can be obtained before collapse occurs? If a hemifusion intermediate is formed, what factors determine if it will productively develop into a full fusion pore and what is the lifetime of such a hemifused state? These aspects of fusion kinetics are of key importance for the proper functioning of a fusogenic system, and any biological situation driving membrane fusion must evolve to form a stable fusion pore of appropriate size.

Two biological solutions for overcoming these energy barriers and traversing the intermediate fusion states have been well characterized structurally and functionally: fusion proteins on the surface of several enveloped viruses and eukaryotic soluble NSF attachment protein receptor (SNARE) proteins. These transmembrane proteins confer fusogenic capacity to the viruses and synaptic vesicles, respectively, that house them. Recent technological advances in fluorescence microscopy have facilitated sensitive and detailed studies of protein-mediated fusion events at the single-particle level, a single particle in this context being a macromolecular object comprised of phospholipids and fusion-mediating proteins, e.g.,

Received: November 22, 2012
Revised: January 26, 2013
Published: February 19, 2013

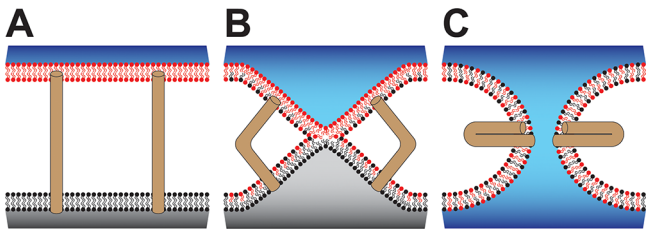

Figure 1. States of protein-mediated membrane fusion that can be accessed by fluorescence microscopy. (A) Two bilayers (red and black) are in close apposition and separate two luminal compartments (blue and gray). Fusion proteins (brown cylinders) in their extended conformation couple the two bilayers and are formed following unfolding of a viral surface fusion protein or v-SNARE−t-SNARE interaction during docking of a synaptic vesicle. (B) The initial refolding of fusion proteins back upon themselves brings sections of the two membranes into yet closer apposition and facilitates the onset of hemifusion, which is an intermediate state characterized by merger of the proximal leaflets from each of the two bilayers. In this state, lipid molecules are able to exchange between the two proximal leaflets, as indicated by mixing of the red and black lipids. (C) Additional fusion protein rearrangements cause full fusion, a state characterized by the merger of the distal leaflets and the formation of a pore connecting the two previously separated compartments to allow content mixing. In the case of viral fusion, pore formation creates a corridor through which the viral genome can pass, while in SNARE-mediated fusion, the fusion pore may be closed before all contents have been released.

enveloped viruses or vesicles incorporating SNARE proteins, which is appropriately labeled for visualization on a fluorescence microscope. Observing individual fusion events is essential for gaining access to the intermediate states visited during membrane fusion and transitions between them. These states are often short-lived and inaccessible to bulk membrane fusion studies, where only average kinetic characterization is possible and individual or rare events are obfuscated. Furthermore, the single-particle-based experimental designs can (partially) overcome technical problems such as vesicle aggregation, bursting, or leakiness that are often obstacles in bulk phase fusion experiments. This review aims to highlight a number of recent experimental methods used to investigate membrane fusion at the single-particle level. These new approaches are allowing direct visualization of fusion intermediates and a probing of stimuli and conditions governing their behavior.

FLUORESCENCE AS A REPORTER FOR FUSION

Fluorescence microscopy has proven to be a revolutionary tool for the study of biological systems by simultaneously allowing real-time observation, a low level of invasiveness, and high specificity. Systems for studying membrane fusion can be based on individual live cells or on purified, individual fusogenic particles (i.e., liposomes or viruses) reconstituted into a controlled fusion scenario. Fluorescent probes used in single-particle fusion studies are typically either small-molecule organic dyes or fluorescent proteins. Organic dyes are frequently used in membrane fusion studies because these can be used to label the lipid−membrane substrates in a straightforward manner. Lipids coupled to bright fluorophores can be mixed with reconstituted lipids when used in vitro and can spontaneously insert into biological membranes, such as those of intact viruses, and reach high local concentrations. Commonly used fluorescent lipophilic probes (Table 1) include long-chain dialkylcarbocyanine dyes such as DiD and DiI and

Table 1. Fluorescent Dyes for Visualizing Membrane Fusion

		Fluorescent Label	Detection Signal *
lipid mixing (hemifusion)	In Vitro	R18	Dequenching [48]
		Rh110 [A]	Dequenching [38]
		TMR-PE or TRITCH-PE	Dequenching [57, 58; D]
		Rh-PE	Dequenching [80] Dissipation [55]
		DiD	Dequenching [11, 12]
		DiD + DiI	FRET increase [84]
	In Vivo	DiD	Dequenching [61] Dissipation [64]
content mixing or release (pore formation)	In Vitro	SRB	Dissipation [38, 48] Dequenching [11, 12]
		Fluorescein	Dissipation [48; B]
		Calcein	Dequenching [10]
		DNA hairpin	FRET decrease [91, 93]
	In Vivo	Palmitylated YFP	Dissipation & Recovery [65; B, C]
		Cleaved GFP fusion	Dissipation [64; B]
		FM1-43	Dissipation [106]
		FM4-64	Dissipation [20]
		Quantum Dots	Fluorescence increase or loss [109; B, C]

[a]Selected references only; not a complete listing. [b]Not commercially available. [c]pH-sensitive, which might be observed when it is used. [d]Not released upon partial pore opening. [e]Reported to visualize both inner and outer leaflet fusion.

dyes having phosphoethanolamine (PE) headgroups such as tetramethylrhodamine (TMR-PE or TRITCH-PE), octadecyl-rhodamine B (R18), lissamine rhodamine B (Rh-PE), or Texas-red-PE (Rh-PE). These lipophilic dyes provide a direct readout for lipid mixing between two bilayers, through dequenching or FRET (Förster or fluorescence resonance energy transfer) (Figure 2). It is of critical importance, however, to realize that lipid mixing is not necessarily a direct readout for full fusion. Full fusion, characterized by a lipidic fusion pore, requires separate fluorescent measurement to detect the transfer of content after the formation of a pore.

Various steps in the fusion pathway can be visualized using fluorescence reporters of lipid and content mixing; three such visualization strategies are depicted in Figure 2. When the lipophilic dyes are incorporated into a bilayer at a sufficiently high concentration, their tight molecular packing can cause quenching of fluorescence by relaxation of an excited dye through a non-photon-emitting process. When labeled and

dx.doi.org/10.1021/bi301573w | Biochemistry 2013, 52, 1654−1668

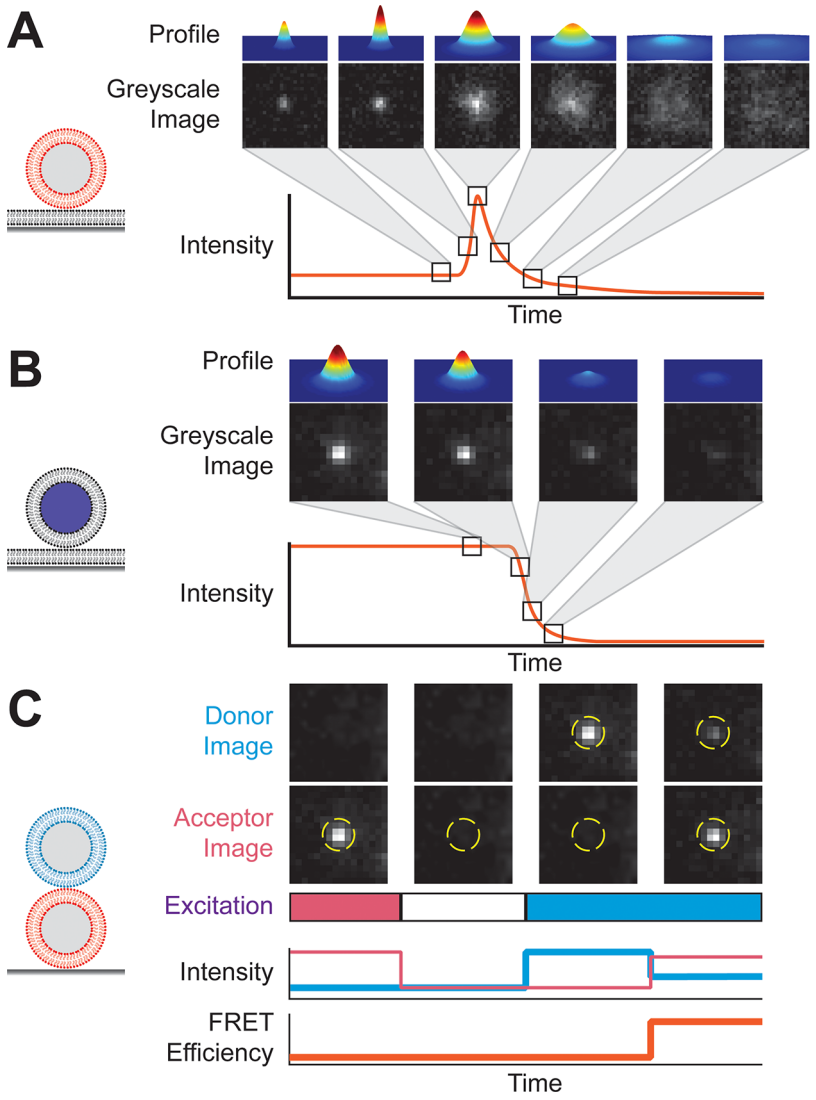

Figure 2. Visualizing membrane fusion through fluorescence signals. Labeled and surface-immobilized fusogenic particles are depicted on the left of each panel. Grayscale images, as captured on a CCD camera, and three-dimensional fluorescence profiles above those images show how the recorded and peak intensity, respectively, of a particle's fluorescence signal change through the time course of fusion at a fusion site. Quantifying the fluorescence intensity present in the CCD images provides "intensity vs time" diagrams. (A) Dequenching upon hemifusion to a large, planar bilayer (black) with outward diffusion of lipophilic dyes (red) from the fusion site. When the dequenching signal arises from content mixing of two vesicles, as described by Kyoung et al.,[11] diffusion away from the site of fusion is not possible. (B) Dissipative fluorescence loss upon escape of an aqueous fluorescence signal (purple) from the lumen of a fusogenic particle through the fusion pore. A similar fluorescence signal is obtained for lipid mixing when dequenching does not occur. (C) FRET-based detection of hemifusion between two immobilized and labeled fusogenic vesicles (red and cyan). Independent excitation of acceptor and donor dyes allows for visualization of each of the overlapping vesicles. Only after fusion is the acceptor vesicle visualized via donor dye excitation, producing a strong FRET efficiency signal.

unlabeled membranes fuse, the lipids rapidly redistribute from the labeled to the unlabeled membrane, decreasing the local concentration of the dye molecules in the labeled membrane. This dilution alleviates the neighbor−neighbor quenching and results in a rapid fluorescence increase known as dequenching (Figure 2A). Detection of this signal is a common indicator of the creation of the hemifusion intermediate and has been described as a "flash".[8] R18, in particular, is a commonly used dye for detecting lipid mixing because it does not rapidly redistribute between closely apposed membranes in the absence of (hemi)fusion and unincorporated dye can easily be removed.[9] The formation of a fusion pore can be directly read out through dequenching of a content label contained within vesicles or liposomes. Calcein[10] and sulforhodamine B[11,12] (Table 1) exhibit a strong degree of quenching at high concentrations, and when the labeled vesicle or liposome contents mix with unlabeled buffer, a dequenching spike similar to that observed for hemifusion can be visualized. Both dyes are charged compounds and can leak from labeled liposomes, so care should be taken to ensure that leakage does not affect experimental outcomes.

The dyes DiD and DiI can be used as a FRET pair (Table 1), wherein the green-emitting DiI is excited by appropriate illumination and its emission is transferred through non-radiative resonance to DiD neighbors, which then emit a photon. This process is highly distance dependent and can be observed as an increase in red emission with a concomitant decrease in green emission once lipid mixing between two apposed membranes has occurred (Figure 2C). This technique

dx.doi.org/10.1021/bi301573w | *Biochemistry* 2013, 52, 1654−1668

Table 2. Novel and Notable Single-Particle Experimental Setups for Visualizing Membrane Fusion

	experimental design		microscope setup	time resolution	advantages	limitations
In vitro	SLB-based membrane fusion	docking under fusogenic conditions	TIRFM [10,47,55]	1−100 ms	simultaneous lipid and content mixing observation	SLB formation, stability, reproducibility
		predocking with fusion trigger	TIRFM [38,48]	100 −1000 ms	simultaneous lipid and content mixing observation; trigger to fusion event time extraction	SLB formation, stability, reproducibility
	tethered vesicle−vesicle fusion	predocking with fusion trigger	TIRFM [11,12,84]	100 −900 ms	simultaneous lipid and content mixing observation; trigger to fusion event time extraction	small number of observations per experiment because of two-body binding
			Confocal [92]	200 −1000 ms	simultaneous lipid and content mixing observation; potentially larger FOV	time resolution depends on the size of the FOV
In vivo	viral tracking within a target cell	temperature- or pH-synchronized fusion	Confocal [64,68]	6 −8 s	trigger to fusion event time extraction[b]; simultaneous lipid and content mixing observation; amenable to labeling of other cellular proteins; three-dimensional tracking; potentially larger FOV	time resolution depends on the size of the FOV; small number of observations per experiment
			epifluorescence/ TIRFM [69,71,72]	0.5 −10 s	simultaneous lipid and content mixing observation; obtain waiting time between trigger and fusion events[b]; amenable to labeling of other cellular proteins	small number of observations per experiment
	synaptic vesicle fusion in live neurons	styryl dye labeling	Epifluorescence [106,110]	15 −36 ms	fluorescent dye can undergo endocytotic recycling; potentially amenable to labeling of other cellular proteins	whole cell, nonspecific labeling; potential for high fluorescence background and phototoxicity
		quantum dot labeling	Epifluorescence [109]	33 −300 ms	direct observation of multiple kiss-and-run fusion events; extended observation with minimal photobleaching	broad quantum dot emission spectra limit labeling of other cellular proteins; quantum dots exhibit higher cellular toxicity than dyes or FP; high phototoxicity at long observation times
		pHluorin-fusion protein labeling	Epifluorescence [111]	9.6 ms	specific labeling of synaptic vesicles by SNARE protein; amenable to labeling of other cellular proteins	high fluorescence background; rapid photobleaching

[a]Selected references only; not a complete listing. [b]Trigger refers either to a synchronizing event or to a change in pH when pH-sensitive FP are attached to virions.[68,69]

is commonly used in bulk lipid mixing studies but has also been applied to single-particle fluorescence microscopy studies.

The advantage of small, organic dyes is their superior photostability and brightness in comparison to those of fluorescent proteins. These benefits generally come with the difficulty of applying them to specifically label a protein or structure of interest in vivo. Techniques for applying this type of labeling are nicely reviewed elsewhere,[13−15] as is the applicability of fluorescent proteins for the labeling of lipid membranes.[16−18] Synaptic and secretory vesicles are exceptions to this generality, however, and the exogenous addition of styryl pyridinium dyes can label these structures in vivo with good specificity and selectivity. These types of dyes rapidly insert into the outer leaflet of bilayers in a reversible fashion and concomitantly exhibit an increase in fluorescent brightness within a bilayer's hydrophobic interstice. Dyes such as FM1−43 and FM4−64 are commonly used to visualize these types of vesicles, which then appear as punctate structures within neuronal or secretory cells. Fusion events are detected as a loss of signal from a fluorescent punctate as the dye molecules

departition from the membrane and both escape through small fusion pores[19] and become dispersed into the plasma membrane.[20] Because the entire plasma membrane is labeled in this technique, there are fluorescent background and potential phototoxic effects that must be taken into account.

Fluorescent proteins (FP) make up for their comparatively poor photostability and brightness with their in vivo specificity. A majority of the common fluorescent proteins are monomeric and can be genetically encoded as in-frame fusions with a protein of interest at either the N- or C-terminus or even within a flexible loop. Recent reviews[21−24] provide detailed overviews of fluorescent proteins and their properties, uses, and pitfalls. One particular characteristic of fluorescent proteins that has been exploited in the study of membrane fusion is their pH sensitivity (Table 1). Generally, fluorescent proteins lose fluorescence brightness gradually as the pH decreases to acidic levels but maintain ∼50% of their brightness down to pH ∼5.0. To leverage this effect for the study of secretory and synaptic vesicle dynamics, Miesenböch et al.[25] engineered green fluorescent proteins to have increased pH sensitivity. Their "pHluorin" mutants displayed a marked change in either the excitation spectrum or fluorescent brightness upon neutralization of an acidic synaptic vesicle following fusion with the plasma membrane.

FLUORESCENCE MICROSCOPY

Common fluorescence microscope designs for the study of membrane fusion kinetics are the epifluorescent and total internal reflection fluorescent (TIRF) microscopes. Both are wide-field microscopy techniques because they illuminate a large field of view (FOV) continuously. Modern electron-multiplying charge-coupled device (EM-CCD) cameras are able to image the fluorescence from large FOVs at high frame rates and with single-molecule sensitivity.

In epifluorescence microscopy, the excitation light propagates through the entire sample, causing fluorescence in any of the vast number of molecules it may come across. This illumination strategy gives great penetration depth for imaging but produces a high background that can quickly degrade the signal-to-background ratio in an image. TIRF microscopy, in contrast, selectively illuminates only a very thin region, with a thickness of approximately 100 nm, immediately above the glass substrate surface. The exclusion of background fluorescence from elsewhere in the sample results in a high signal-to-background ratio for fluorescent molecules within the excitation volume at the expense of a low penetration depth. The physical explanation for this effect and guidelines for construction of a TIRF microscope are nicely described elsewhere.[26−28] TIRF microscopy is particularly useful for the study of membrane fusion events because the plasma membrane of many cell types can be brought within the TIR illumination volume. Confocal microscopes can also be used, where the light is focused into a diffraction-limited volume or "spot" rather than illuminating a large volume of the sample. Images are obtained by raster-scanning the confocal volume throughout a defined FOV, and the fluorescence information is collected with a photomultiplier tube or photo diode. Fluorescence emanating from outside the focal volume of interest is eliminated to provide images with a high signal-to-noise ratio and low background. Even though full images are acquired at a much lower time resolution, the signal from one particular spot can be followed with sampling rates orders of magnitude higher than that with wide-field imaging techniques.

These microscopy techniques allow for a range of temporal resolutions (Table 2), but the spatial resolution is generally dictated by the diffraction limit of ∼300 nm. If sufficient photons are collected and the fluorescent particle is a point source with dimensions smaller than the diffraction limit, then the particle's position can be determined to ∼1−2 nm accuracy,[29] which is useful for particle tracking. Super-resolution imaging (i.e., STORM, PALM, etc.; reviewed in ref 30) could be used in conjunction with single-particle tracking to precisely localize fusion events within a cell, though this has yet to be demonstrated.

SUPPORTED LIPID BILAYERS

Many in vitro studies of membrane fusion make use of artificial lipid bilayers supported by a solid substrate. Several techniques exist to construct these supported lipid bilayers (SLBs) and have recently been reviewed for a wide range of applications by Czolkos et al.[31] and Richter et al.[32] For the purposes of microscopy, they are formed upon the surface of a cleaned, hydrophilic glass or quartz substrate and, in many cases, can allow for the incorporation of functional transmembrane proteins. The most common techniques for forming SLBs are vesicle rupture and self-spreading[33] and successive transfer of two phospholipid monolayers using a Langmuir−Blodgett approach.[34] In its simplest implementation, the former technique requires incubation of a lipid solution with a solid, hydrophilic support, while the latter is more involved and involves sequential transfer of the two phospholipid monolayers. SLBs can also be formed upon a polymer cushion [such as polyethylene glycol (PEG)[35,36]] or tethered to the solid substrate (such as with DNA[35,37]) with the goal of creating a (mostly) aqueous volume that entirely separates the bilayer from the substrate's surface. High-molecular weight dextran has also been used as a cushion suitable for conducting single-particle viral fusion experiments,[38] expanding on a technique that had been previously reported.[39] The practical difficulty in reproducibly creating fluid and continuous SLBs using these methods necessitates further work in optimizing surface chemistry.

VIRAL MEMBRANE FUSION

Influenza hemagglutinin (HA) is the most intensively investigated of all the viral fusion proteins. The structural and functional aspects of HA have been thoroughly discussed in several publications.[40−43] Briefly, HA is a class I trimeric fusion protein, with each monomer containing the two disulfide-linked HA1 and HA2 domains. HA thereby combines the domains responsible for receptor binding (HA1) and fusion (HA2) into a single protein machine. During clathrin-mediated endocytosis, the HA2 domain responds to acidification of the endosomal lumen by undergoing a conformational unfolding into an extended rod-shaped protein consisting of a three-helix bundle of coiled α-helices. The critical pH for this unfolding step is ∼5.5 for most influenza strains. Unfolding exposes the hydrophobic N-terminus of HA2, termed the fusion peptide, which inserts into the proximal leaflet of the target bilayer. When HA2 refolds back upon itself, the fusion peptide serves as an anchor to bring the target membrane into the proximity of the viral envelope. This action facilitates fusion of the proximal leaflets of the two bilayers (Figure 1) into a hemifusion structure. The distal leaflets are merged by subsequent rearrangements of the HA2 transmembrane domain, thereby

creating a fusion pore for the escape of viral contents into the cellular cytosol. The three major classes of viral fusion proteins are all trimeric in their fusion-active state and are thought to follow the overarching scheme described here for HA.[42] The unfolding event is not necessarily pH-dependent, though, and can occur at neutral pH values for some virus types. While these structural rearrangements required of HA2 and other fusion proteins to mediate fusion are widely accepted, there is much debate regarding the number of activated trimers on the viral surface required to act in concert for the fusion process to occur.

SINGLE-PARTICLE VIRAL FUSION KINETICS STUDIED IN VITRO

Several decades of fluorescence microscopy studies of HA-mediated fusion have contributed significantly to our understanding of the intermediate states and molecular processes that occur en route to viral membrane fusion. These studies have principally implemented two strategies: cell−cell fusion using HA-expressing cells and single-particle virus−target or virosome−target fusion. In the single-particle context of this review, we will focus on the latter of these techniques, though this is not to downplay the many insights into HA fusion and membrane fusion in general provided by fluorescence microscopy studies of cell−cell fusion.

Target membranes used to study HA-mediated fusion (Figure 3A,B) at the single-particle level are formed by different techniques. The earliest single-particle studies used intact erythrocytes[44,45] or black lipid membranes (BLMs)[8,46] as targets for fusion. A BLM is a small circular patch of lipid bilayer painted onto a small hole in a Teflon sheet that serves as an aperture to support the bilayer at its edges. More recent studies were based on the formation of glass- or quartz-supported lipid bilayers through incubation with vesicles,[38,47,48] as described above, or on the immobilization of erythrocytes to a glass surface and their subsequent rupture, leaving an adhered cellular SLB.[49]

Intact and infectious influenza virions can be readily labeled with high concentrations of the self-quenching red-emitting dye R18[50] without compromising infectivity. A similar octadecylrhodamine 110 (Rh110), a green-emitting lipophilic dye, has also been used to monitor hemifusion,[38] though it is not commercially available. Viral contents can be exogenously labeled with sulforhodamine B (SRB)[38] or with pH-sensitive fluorescein[48] by overnight incubation of the virus particles with high concentrations of the dyes. Loss of these content signals during the fusion process (Figure 3B) indicates the opening of a fusion pore large enough for the dye molecules to pass through (SRB or fluorescein) or the acidification of the viral lumen (fluorescein). HA-mediated fusion events are visualized by first immobilizing the intact and labeled virus onto the target membrane, followed by synchronously inducing fusion through a rapid pH decrease (Figure 3B). Kinetics are extracted as the elapsed time between acidification and the dequenching event for hemifusion or the time passed between the pH decrease and the loss of content fluorescence for pore formation or acidification.

Floyd et al.[38] found that with a decrease in pH from neutral to a range of 4.5−5.3 the rate of hemifusion rapidly becomes faster with a lower target pH. When the pH is lowered below 4.5, the rate of hemifusion plateaus and is no longer pH-dependent. These results confirm a trend initially described by Niles and Cohen[46] but do so with greater sensitivity, greater

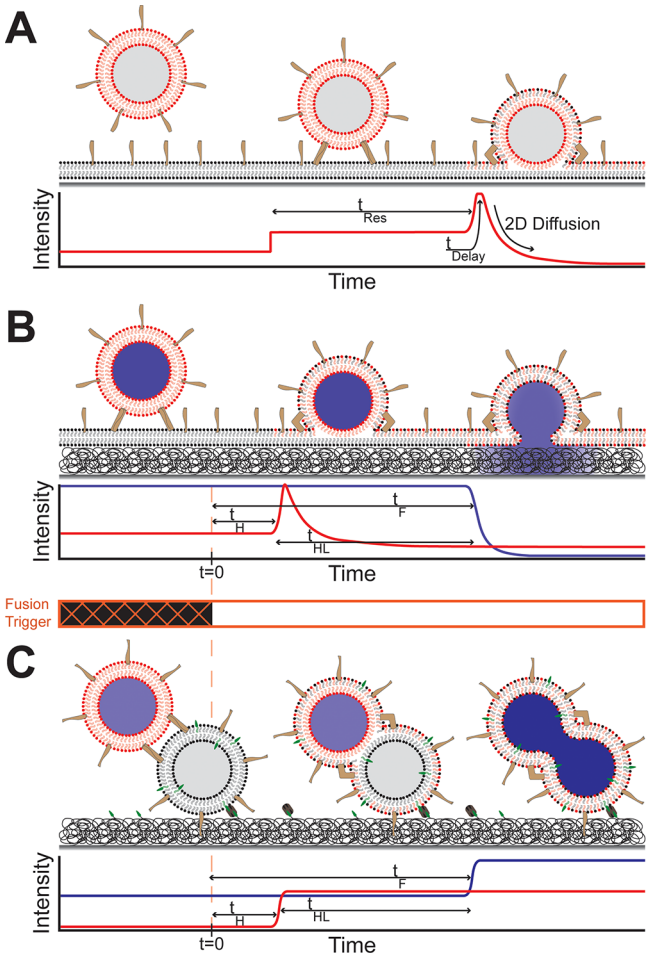

Figure 3. Observing membrane fusion in vitro utilizing fluorescence. Fusogenic proteins are drawn as light brown half-cylinders, and docking elements, such as t-SNARE proteins or receptor molecules, are drawn as complementary half-cylinders. Lipophilic dye labeling is colored red and content labeling purple. (A) Observation of the transitions from particle docking to hemifusion as implemented by Wessels et al.[47] and others.[10,55−58] The following kinetics were obtained: the residency time between docking and the dequenching fusion signal, t_{Res}; the two-dimensional diffusion constant of the lipophilic dye away from the site of fusion; and, in some instances, the time between fusion and the onset of outward dye diffusion, t_{Delay}. (B) Transitions from triggering fusion to full fusion with a polymer cushion-supported (black mesh below lipids) planar bilayer as implemented by Floyd et al.[38] The following kinetics were obtained: time between fusion trigger and hemifusion, t_H; the time between trigger and full fusion, t_F; and the time between hemifusion and full fusion, t_{HL}, which is the lifetime of the hemifused state. (C) Transitions from triggering fusion to full fusion to an immobilized target vesicle as implemented by Kyoung et al.[11] In contrast to panels A and B, immobilization is achieved through avidin (brown rectangles)−biotin (green cones) interaction rather than through a fusion-related interaction. Accessible kinetics are similar to those in panel B.

delineation of receptor binding and fusion, and more robust statistics. In the experiments by Floyd et al., the onset of acidification was directly read out as a loss of the fluorescence signal from a buffer-exposed pH-sensitive fluorescein dye that was bound to the target membrane. The waiting-time distributions between the pH decrease and the onset of hemifusion showed a clear rise and decay, indicative of multiple biochemical intermediate steps.[51,52] Modeling the waiting times

dx.doi.org/10.1021/bi301573w | Biochemistry 2013, 52, 1654−1668

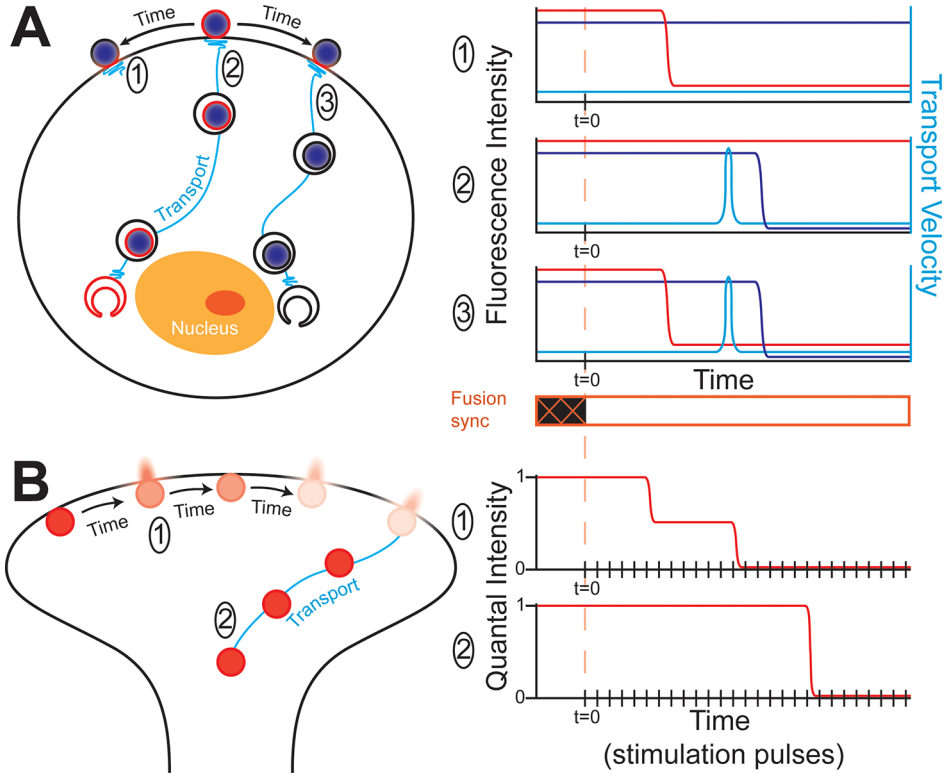

Figure 4. In vivo visualization of membrane fusion during viral infection and synaptic firing. (A) Lipid mixing and content release during viral infection as utilized by Miyauchi et al.[64] and described in the text. The lipophilic dye for monitoring membrane mixing is colored red, content labeling purple, and the velocity of viral movement light blue. Dual-labeled viruses first bind to the target cell at the start of path 2. Once fusion is synchronized, the virus may undergo hemifusion with the plasma membrane via path 1 or 3, or with the endosome via path 2 or 3 that releases the viral contents into the target cell. (B) Subquantal and full quantal content release during synaptic vesicle fusion based upon the experimental design of Aravanis et al.[106,107] The fluorescence from FM1−43 is colored red, and stimulatory pulses are indicated as vertical hashes in the intensity diagrams. Path 1 depicts kiss-and-run fusion with multiple events, and path 2 depicts the full fusion event without a prior kiss-and-run fusion. Synaptic vesicle transport was not directly followed by particle tracking; rather, it was inferred from the fusion kinetics. Quantum dots report kiss-and-run fusion events through a small fluorescence increase[109] rather than a signal loss.

with a gamma distribution allowed for an estimation of both the velocity of the rate-limiting step in the process and the number of rate-limiting steps that are required for hemifusion to occur. While the rate of fusion in the pH-dependent regime varied from 0.03 to 0.3 s^{-1}, the number of rate-limiting steps remained constant at approximately three. This result was interpreted to be that three HA trimer molecules are required to undergo conformational unfolding and refolding to mediate hemifusion.

A requirement for three HA trimers to undergo a conformational change and coordinate their actions for fusion to occur was in agreement with theoretical estimates,[53] which were based on electrical admittance measurements for fusion of HA-expressing cells with a SLB.[54] A previous study by Imai et al.[49] followed the hemifusion kinetics in a similar fashion while varying the concentration of fusion-active HA present on the surface of reconstituted virosomes. With the assumption that assembly of a number, n, of fusogenic HA trimers would be the rate-limiting step in the kinetics, they fit their data to the function $V = k[HA_{1,2}]^n$, where V is the fusion rate and k is a constant, to obtain an n of 0.9 ± 0.4. They interpreted this to indicate that a single HA trimer was necessary and sufficient to mediate fusion, though the waiting-time distributions between acidification and hemifusion showed clear rise-and-decay characteristics. A subsequent reanalysis of their waiting-time distributions[59] found that their kinetic data were identical to those of Floyd et al.[38] and corroborated the need for three HA trimers to undergo conformational refolding. Unfolding of the HA trimer (i.e., the loop-to-helix transition) has been calculated to liberate ∼125 k_BT (75 kcal/mol) of free energy.[60] If three trimers unfold, only a fraction of the total free energy liberated would need to be recaptured to overcome the initial energetic barrier to hemifusion.[42]

Wessels et al.[47] observed hemifusion of influenza and Sindbis (an alphavirus with a pH-sensitive Class II fusion protein) viruses by first mixing them with acidic solution and then exposing them to a target bilayer lacking receptor molecules (Figure 3A). In this experimental configuration, the fusion proteins unfold in the absence of a bilayer. Exposure of their hydrophobic fusion peptide/loop causes them to briefly immobilize upon the bilayer just prior to folding back and fusing. The viruses were found to differ in residency time between bilayer interaction and fusion. For influenza, the residency time was constant regardless of the conditions. For the Sindbis virus, on the other hand, the residency time varied as cholesterol and sphingomyelin were added to the phosphatidylcholine/phosphatidylethanolamine target bilayers. Separately, the Sindbis residency time also varied with pH, increasing 5−10-fold as conditions were progressively made more acidic. Hence, viruses can exhibit varied kinetic behavior and dependencies starting from a situation in which the fusion proteins have already unfolded and only fold-back is necessary.

The completion of fusion by the opening of a full fusion pore, allowing viral content release, was also studied by Floyd et al.,[38] who employed a dual-labeled virus (rhodamine-110 lipid

dx.doi.org/10.1021/bi301573w | *Biochemistry* 2013, 52, 1654−1668

dye in combination with SRB content dye). The aforementioned hemifusion kinetics were used in conjunction with the waiting time between acidification and content signal dissipation to probe the lifetime of the hemifused state that exists prior to the opening of a full fusion pore (Figures 1B,C and 3B). They found that lipid mixing preceded content release and the elapsed time between the two events as measured for individual particles provided a direct measure of the hemifusion lifetime. The dwell-time distributions for these lifetimes were described well by a single-exponential distribution for the full pH range of 3.5−5.3, indicating that only a single rate-limiting step gave rise to full membrane merger after hemifusion was established. Importantly, the transition from the hemifusion intermediate to pore opening is difficult to access by bulk fusion techniques.

A recent study using viral content labeling by Ivanovic et al.[48] compared the rate of SRB signal loss to that of signal loss from the pH-sensitive dye fluorescein. The latter allowed for a measurement of the kinetics of acidification of the viral lumen, mediated by the influenza integral membrane proton pump, M2. Acidification of the viral interior is a critical step for release of the viral genome from the structural matrix protein, and internal acidification was hypothesized to take place prior to fusion. Two time points were identified in the single-particle acidification study: the time to onset of internal virus acidification following the external pH decrease and the time from the onset of internal acidification to loss of half the fluorescent signal, termed the dissipation time. The times to onset and to dissipation were compared for the fluorescein and SRB content label and showed that internal viral acidification precedes fusion pore opening, occurring on average ∼100 s earlier at a target pH of 4.5. Using the dissipation time of the fluorescence signal, the authors estimated that the M2 channel transferred between 100 and 400 protons/s into the viral lumen prior to pore opening. Adding the M2 channel-blocking molecule Rimantadine caused the fluorescein loss to become kinetically indistinguishable from the SRB loss, suggesting that with inhibited M2, internal acidification took place only after pore formation. Further, the kinetics of SRB loss were indistinguishable from those measured in the presence of fully active M2 proton channels. This observation established that there was no effect of acidification of the matrix on the kinetics of pore formation.

SINGLE-PARTICLE VIRAL FUSION KINETICS IN LIVING CELLS (IN VIVO)

Visualization of the fusion between a virus and a cellular target in living cells (in vivo) provides insight into how viral fusion proteins mediate fusion during the initiation of infection in their intended environment. Of great interest and importance are the cellular location where and the conditions under which membrane fusion occurs for the infection process to functionally begin. These initial steps are well-characterized for some viruses, such as influenza, while they are contested for others, such as HIV-1. It is advantageous that in these studies the virus is necessarily added exogenously and so can be labeled and manipulated in a manner that is independent of the target cellular system. The bright lipophilic dye DiD is often used to label the envelope of a number of viruses types, such as influenza, HIV, murine leukemia virus (MLV), and avian sarcoma leucosis virus (ASLV). In some cases, it is incorporated to a degree sufficient for dequenching upon membrane fusion[61−63] or can report fusion through disappearance of the fluorescent signal upon near infinite dilution into large cellular membranes.[64−66]

Measuring fusion kinetics requires a synchronization time point from which the time until lipid mixing (hemifusion) can be measured (Figure 4A). A sudden temperature jump starting in a range of 4−18 °C and rising rapidly to 37 °C has served as the synchronization in numerous experiments.[61,64,67,68] Acidification of the extracellular buffer can force pH-dependent viral fusion at the plasma membrane.[65] Alternatively, incubation with ammonium chloride can be used to neutralize all cellular compartments followed by its removal to allow endosomal acidification, thus synchronizing the fusion of internalized virions.[69] Acidification of individual endosomes harboring and transporting viruses can be directly measured by incorporating transmembrane domain-associated GFP proteins to the viral envelope.[68,69] Detection of a pH decrease and subsequent fusion allows for direct kinetic measurements to be made en route to infection, akin to in vitro measurements for extraction of pH dependencies.

Tracking the location of a labeled virus particle has provided valuable information regarding entry, subsequent trafficking, and egress of new virus particles. These results have been reviewed by Brandenburg and Zhuang,[70] along with a discussion of additional labeling techniques and pitfalls. The relevance of trafficking behavior to viral membrane fusion was first described by Lakadamyali et al.,[61] who followed the movement of intact influenza virus following endosomal internalization. The authors describe a three-stage transport process in which the virus is first bound to the cell periphery with a low degree of mobility and then suddenly undergoes a unidirectional, rapid movement toward the cell nucleus (Figure 4A). This transport behavior is most often tightly coupled with clathrin-coated pit formation.[62] Finally, the virus experiences intermittent back-and-forth movement, finally terminating in membrane fusion with the endosome in the perinuclear region of the cell.

Trafficking of intact dengue virus[63] and ASLV-Env pseudoviruses[66,68] also gave rise to such a three-stage transport behavior, indicating it may be a general pathway followed by viruses during endocytosis. Pseudoviruses are particles having surface proteins from one virus type and a core from a second virus type, for instance, HIV-1 Env fusion proteins with a MLV core of matrix proteins with the associated genome.[67] Concomitant labeling of the early and late endosomal markers Rab5 and Rab7, respectively, provides information regarding the particular stage of endosomal maturation during which membrane fusion is most likely to occur.[69,71] Single-particle tracking has also shown that the surface receptor to which a virus first binds a target cell can directly affect subcellular transport, the rate of fusion, and the compartment where the viral core is released.[66,68,69]

To assess infection with single-particle fluorescence assays, it is necessary to separately and simultaneously measure the release of viral contents. Such observations allow for detection of intermediates along the fusion pathway, such as hemifusion and small, nascent fusion pores. Melikyan and colleagues have developed several strategies for detecting content release by incorporating pH-sensitive fluorescent proteins into the lumen of a number of pseudoviruses. One such pseudovirus was constructed to have a palmitylated YFP coating the luminal leaflet of the viral membrane.[65] Small, transient fusion pores were observed to allow mixing between viral contents and the cytosol, but without release of the lipid-bound protein from

within the virus. Half of these small and nonexpanding fusion pores had surprisingly long lifetimes, lasting for tens of seconds and, for some, as long as several minutes. The size of the fusion pore can also be dependent upon the receptor used by the virus and the compartment in which fusion occurs.[66,68] These observations indicated that pore expansion could be a significant energetic barrier to infection following hemifusion.

Another method used with several pseudoviruses involves use of the MLV Gag protein fused to a GFP in such a way that when the Gag is cleaved during viral maturation, it becomes a freely diffusing fluorescent viral content marker.[64,66−69,72] A recent study using this type of pseudovirus[64] provided strong support for the idea that the pH-independent HIV-1 Env proteins mediate an endosomal route for viral entry and fusion, similar to pH-dependent viral surface proteins like HA. Miyauchi et al.[64] followed the fusion pathway through the disappearance of either the DiD envelope dye, which indicated hemifusion with the cellular plasma membrane, or the GFP content marker, which indicated content release (Figure 4A); fusion with an endosome resulted in a persistent DiD signal and loss of the content signal. Using a number of HIV-1 pseudoviruses and one fully infectious strain, they observed many viruses fusing with the plasma membrane, but not losing their contents (Figure 4A, 1), while others had a persistent lipid signal and a rapid content loss (Figure 4A, 2). Importantly, the viruses exhibiting plasma−membrane hemifusion often showed limited movement, while those losing their contents showed transport toward the cell nucleus before content loss and a continued movement of the lipid dye afterward, observations consistent with endosomal trafficking and perinuclear viral genome release. Very few viruses showed loss of both signals (Figure 4A, 3), with a considerable delay separating content release from lipid mixing. The delay time between lipid mixing and content release was consistent with the time measured as being necessary for endocytosis (10−15 min). These observations were supported with experiments providing a cellular readout to indicate successful viral core transfer. Moreover, a long-lived intermediate state following HIV-1 Env-mediated lipid mixing and preceding content loss had been reported previously,[67] consistent with the observations of Miyauchi et al.

As further evidence of HIV-1 endosomal uptake and fusion, Miayuchi et al.[64] and a follow-up study by de la Vega et al.[72] showed that inhibition of the dynamin GTPase (the protein responsible for scission of clathrin-coated pits from the plasma membrane during endocytosis) abolished viral content release but did not inhibit lipid mixing with the plasma membrane. Together, these studies indicated that the HIV-1 Env fusion protein can mediate the transition into a long-lived hemifusion state with the plasma membrane before the virus is internalized, but that a functional fusion pore is not created at the plasma membrane, rather within the endosome.

Taken together, these studies demonstrate that the intermediates in viral fusion as derived from biophysical, biochemical, and structural data are experimentally resolvable at a single-particle level. The kinetic insight obtained with these studies has contributed significantly to our understanding of the molecular mechanisms by which fusion proteins catalyze fusion. Moreover, additional processes, such as acidification of the viral lumen, can occur in parallel with traversing of the intermediate physical states leading to membrane fusion. Results also indicate that there is coordination between viral surface proteins that must occur for membrane fusion to occur and that the kinetics for coordination vary with pH regime. Within a cellular context, endosomal trafficking and maturation appear to provide receptor-dependent pathways for productive viral fusion. Such a deep understanding of the molecular nature of fusion intermediates may prove to be crucial in relating in vivo and in vitro observations as well as to developing novel antiviral therapeutics that neutralize specific intermediates along the fusion pathway .

SNARE-MEDIATED MEMBRANE FUSION

Recently, fluorescence microscopy has also been applied extensively to the study of fusion of membranes driven by the SNARE machinery in eukaryotes. SNARE proteins are responsible for the fusion of synaptic vesicles with the neuronal plasma membrane, supporting rapid action potential-triggered exocytosis of neurotransmitters into the synaptic cleft. The function of these proteins has been the subject of thorough and recent reviews by Brunger and colleagues;[73,74] only a brief outline of how they mediate fusion is given here.

The SNARE proteins are divided into two groups: target SNARE (t-SNARE) proteins anchored to the luminal side of the plasma membrane and vesicle SNARE (v-SNARE) proteins anchored to the synaptic vesicles, which contain neurotransmitters. The principal t-SNARE proteins are syntaxin-1 (Syx) and SNAP25, while synaptobrevin-2 (Syb, also known as VAMP, vesicle-associated membrane protein) is the principal v-SNARE. Together, these three proteins are considered the functional core responsible for mediating membrane fusion. Synaptotagmin-1 (Syt) and complexin are two important protein factors that interact with the SNARE proteins and have been incorporated into single-particle SNARE fusion studies; factors Munc13 and Munc18, though critical for vesicle priming,[75] have not yet been included in such studies. Syt is the calcium (Ca^{2+}) sensor required for fast synchronous release of neurotransmitters, and complexin is a modulator regulating SNARE-driven exocytosis. For fusion to occur, SNARE proteins first associate with each other to form a tetra-α-helix complex comprised of two SNAP25 proteins, one Syx, and one Syb that, together, link the v- and t-membranes in the proximity of each other. In response to a rapid influx of Ca^{2+} ions into a neuron following the arrival of an action potential, the SNARE proteins refold upon each other in a fashion enhanced by the concerted action of additional protein factors. These interactions bring the apposed membranes into close proximity and facilitate their fusion, releasing neurotransmitters into the synaptic junction for action potential propagation.

Neurotransmitter release has been demonstrated to occur in as little as 0.2 ms following an action potential.[76] Additionally, neurons can be required to transmit high-frequency signals rapidly and continuously. There are two principal modes by which a vesicle can fuse during exocytosis. One is complete fusion, where the vesicle fully collapses to become continuous with the plasma membrane and simultaneously releases its entire contents.[77] These vesicles are replenished by de novo synthesis coupled with endocytotic recycling. Alternatively, there is "kiss-and-run" fusion where the exocytotic vesicle does not undergo complete fusion but rather releases a portion of its contents followed by fusion pore closure.[78] The kinetics and intermediates involved in both modes of fusion are amenable to fluorescence microscopy, and their study paints a picture of the bilayer rearrangements and vesicle cycling that occur during action potential propagation.

SINGLE-PARTICLE SNARE FUSION KINETICS STUDIED IN VITRO

In vitro studies attempting to reconstitute the SNARE fusion process have traditionally been performed using bulk lipid mixing assays. Recent investigations are moving these studies onto the microscope to observe the vesicles fusing individually. Single-vesicle fusion studies have the advantage over ensemble-averaging experiments in their ability to directly differentiate full fusion and content mixing from hemifusion and lipid mixing. This differentiation avoids the misinterpretation of implying content mixing by only monitoring lipid mixing, a potential pitfall discussed elsewhere.[12,79] In addition, these studies can clearly distinguish docking of a v-SNARE vesicle to a t-SNARE membrane from the subsequent fusion event. Docking is observed as the rapid increase in fluorescence from the background at a localized spot as the vesicle becomes immobilized upon the target surface. Lipophilic dyes used in vitro for labeling the vesicle bilayer are often PE-modified lipids such as TMR-PE/TRITCH-PE,[57,58] R18,[10] and Rh-PE.[55,56,80−83] These dyes can indicate lipid mixing through fluorescence dequenching (Figure 2A). Alternatively, DiD and DiI can be used to follow lipid mixing measured as an increase in the level of FRET[84−87] (Figure 2C) or as a dequenching signal.[11,12] Here, we discuss in detail two experimental geometries developed for observing the fusion reaction as mediated by SNAREs: one using a planar SLB target and the other using tethered target vesicles.

A planar SLB formed upon a hydrophilic quartz, glass, or polymer substrate allows observation of SNARE-dependent fusion between the SLB and individual fusogenic vesicles (Figure 3A,B). The t-SNARE proteins are typically contained in the target planar SLB, while the v-SNARE protein is present in small unilaminar vesicles (SUVs) that bind and subsequently fuse to the SLB. The dequenching signal from lipid dye in the v-SNARE vesicles is a common readout for lipid mixing because dilution of the dye into the SLB can easily be visualized. The contents of these vesicles have been filled with fluorescent dyes such as calcein,[10,88] which reports on the opening of a fusion pore through dequenching followed by fluorescence signal loss. The continuity of the SLB can be monitored within the experimental setup by labeling the SLB using NBD-PE[80,81,83] and performing FRAP measurements immediately prior to fusion experiments. Fusion kinetics are measured as the elapsed time between docking and dequenching and require rapid image acquisition, with frame acquisition times as low as 1−5 ms[10,55] (Figure 3A).

A consensus remains to be established for the results produced from planar SLB-based experiments. Fusion was observed in some experimental setups in the absence of the in vivo obligate protein SNAP25[10,58,88] and in the absence of Ca^{2+}.[55,58,88] Bowen et al.[88] demonstrated that the fusion they observed was the result of laser-induced heating, though this may not be the case for the other works cited. Their data also indicated that SNAP25 was required for the formation of a stable interaction between Syx and Syb prior to fusion. However, a number of key observations were shared between SLB-based studies. Hemifusion to the SLB was found to occur 5−20 ms after docking to the bilayer.[10,55,56] Release of a content dye to indicate full fusion was found to occur ∼100 ms after lipid mixing, but this observation was convoluted with vesicle rupture that released the content dye into the space above a SLB rather than below it.[10] Using polarized laser illumination in a TIRF microscope, Kiessling et al.[56] observed the changes in the topology of the vesicle bilayer as it fused with the planar target. They found that the vesicle becomes flattened along the substrate only 8 ms after fusion begins. While fast, these kinetics are still much slower than the 0.2 ms response observed in living cells.[76] Phospholipid headgroups and their ratios appear to have an effect on both docking and fusion efficiency, but there are still differences reported between different experimental designs and setups (discussed in ref 82). Finally, SLB-based single-particle studies have estimated that 5−10 SNARE complexes are needed to induce fusion,[55,83] though estimates of as many as 15 complexes exist in the literature.[89] A bulk fusion study measuring only lipid mixing without content mixing found, in contrast, that a single SNARE complex could give rise to lipid mixing.[90]

In the tethered vesicle experimental approach, first developed by Yoon et al.[84] (Figure 3C), separate populations of v- and t-SNARE-containing vesicles are observed while they are fusing together. Either v-SNARE[84−86,91] or t-SNARE[11,12] vesicles are immobilized upon a substrate with no preference in terms of effect.[87] Glass or quartz substrates are coated with a PEG/biotinylated PEG layer to reduce the number of nonspecific interactions, wherein the sparse amounts of biotin-PEG allow vesicle immobilization through neutravidin-mediated binding with biotinylated lipids in the vesicles. Lipid mixing is observed via TIRF microscopy as a FRET signal between DiI and DiD (Figure 2C), though scanning confocal microscopy has also been used.[92] Fusion pore opening can be followed through dequenching of SRB[11] without outward dissipation. A novel strategy for following the expansion of a fusion pore utilizes a DNA hairpin encapsulated in the v-SNARE vesicles.[91,93,94] The hairpin is labeled at both ends such that when it folds upon itself, the two FRET pair dyes are in the proximity of each other and give a strong FRET signal. Upon expansion of the pore, a complementary DNA strand present in the t-SNARE vesicles binds to and opens the hairpin, alleviating the donor dye quenching on a time scale much faster than that of pore expansion kinetics[91] and indicating that the vesicles are joined by a fusion pore at least 2 nm in diameter.[93] This labeling strategy allows for separation of lipid mixing, nascent pore opening, and subsequent pore expansion.

The tethered vesicle experimental geometry has recapitulated some of the requirements and observations seen in in vivo neuronal SNARE fusion. Specifically, the Ca^{2+} inductio-n[11,12,85,93] and SNAP25[12,85,87] dependency of fusion has been reproduced by several groups. In addition, the hemifusion intermediate has been interpreted from the FRET efficiency data of lipid mixing.[84,85,93] Lipid mixing after docking of one vesicle to another showed heterogeneity with two kinetic populations. When coupled with the SNARE-related factors complexin and Syt, the time constant for lipid mixing of the fast population was typically in the range of 100−950 ms.[11,12,85,86,92] These times are likely upper bounds on the fast population set by the experimental equipment used, because the video acquisition rate was lower than that achieved in the planar SLB experiments.[11,12] The slower kinetic component was on the order of 3−10 s and occurred upon Ca^{2+} triggering of the SNARE proteins in the absence of the complexin and Syt factors.[11,85] In agreement with these kinetic measurements, docking was found to be the rate-limiting step in the SNARE fusion process.[87,92] Docking kinetics between complementary SNARE vesicles were found to be enhanced

dx.doi.org/10.1021/bi301573w | Biochemistry 2013, 52, 1654−1668

10−100-fold by the SNARE-related factors complexin and Syt.[11,85,92]

Of particular note, Kyoung et al.[11] enhanced the tethered vesicle design to include a SRB content label for the v-SNARE vesicles, which allows for direct readout of content mixing, as well as a Cascade Blue fluorescent signal to indicate the arrival of the fusion-inducing Ca^{2+} solution (Figure 3C). Within the tethered vesicle design, they successfully reproduced fast content release kinetics on the millisecond time scale that was both Ca^{2+}-induced and dependent on the presence of both complexin and Syt. Extraction of waiting times between Ca^{2+} arrival and hemifusion or content release allowed for a kinetic analysis of the fusion process. They found that in the presence of the Syt and complexin factors, a "rapid burst" constituting simultaneous lipid and content mixing was prevalent. This phenomenon was characterized by a waiting-time distribution for both fluorescent signals that was described well by a double-exponential function, indicative of two populations with each displaying different kinetics. The rapidly fusing portion constituted a majority of the vesicle population and displayed a fusion time constant of 250 ms, approximately equal to the frame rate used to capture the fusion movies. Because of this experimental limitation, intermediates between lipid mixing and content release were not observable. The slower portion of the population displayed a time constant of ∼1.5 s. Without Syt and complexin, however, the SNARE proteins alone could not efficiently generate these rapid bursts or the two kinetic populations. Instead, the waiting-time distributions were described by a single-exponential function with a rate constant of ∼3 s. A subsequent study by Diao et al.[12] used a similar experimental design with a more physiological Ca^{2+} concentration of 250 μM and a shorter frame exposure time of 100 ms but still did not resolve an intermediate state between lipid and content mixing. Addition of the complexin protein enhanced the rapid bursting behavior and the emergence of two kinetic populations of fusing vesicles. In the presence of SNARE and Syt proteins only, however, a larger number of long-lived hemifusion intermediates that did not evolve into full fusion end points were observed.

Enhancement of productive fusion pathways by accessory proteins is supported by recent tethered vesicle experiments conducted by Lai et al.[93] Therein, the authors report that the Syt protein interacts with SNARE proteins to significantly enhance vesicle docking, hemifusion, and the opening of a nascent pore large enough for SRB molecules to pass through. Moreover, using the aforementioned FRET-labeled DNA hairpin, they found that pore expansion is 13-fold slower than nascent fusion pore opening and that expansion is very inefficient in the absence of Syt or Ca^{2+}. Incorporating complexin into the fusion scheme caused the rate of nascent pore opening to increase 21% and the rate of pore expansion to double. Thus, productive fusion pore opening and expansion are modulated, at least, by the accessory proteins Syt and complexin, which can enhance full fusion in terms of both rate and efficiency.

SINGLE-EXOCYTOTIC VESICLE FUSION IN LIVE HIPPOCAMPAL NEURONAL CELLS

Fluorescence microscopy-based kinetic measurements have also proven to be insightful for the in vivo study of exocytosis. Methods for fluorescently labeling exocytotic vesicles in living cells are well reviewed elsewhere by Ge et al.[95] and Keighron et al.[96] These methods have been implemented in monitoring processes closely related to exocytosis, such as endocytosis,[97,98] the role of other key cellular components in exocytosis,[99] and nonsynaptic exocytosis.[100−103] For the sake of continuity with the previous section, the following discussion will focus on synaptic exocytosis in hippocampal neurons and primarily on the kinetic discernment between kiss-and-run fusion and complete fusion wherein the synaptic vesicle fully collapses.

Synaptic vesicles are commonly labeled with organic styryl dyes, such as FM1−43, that have proven to be powerful tools for studying exocytosis in living cells.[95,96] For instance, FM1−43 was used to determine that one-third to one-fourth of the vesicles at the synapse are located in the proximity of the plasma membrane and belong to a readily releasable pool of vesicles, while the remaining vesicles belong to a recruitable reserve pool more distal from the synapse.[104,105] As mentioned previously, these dyes exhibit enhanced fluorescence in hydrophobic environments but also reversibly departition from membranes into the aqueous vesicular lumen. This behavior allows the dissipation of the dye signal to report on the formation of a fusion pore rather than lipid mixing. Aravanis et al.[106,107] used FM1−43 in hippocampal nerve cells, where exocytotic vesicles are clustered into synaptic boutons of approximately 30 vesicles. Using a minimal labeling protocol, they observed individual synaptic vesicles using epifluorescence microscopy. Consistent with other reports of this system,[97,108] each vesicle contained a "quantal" amount of dye such that the fluorescent signals from individual vesicles were comparable. Fusion of individual vesicles to the plasma membrane was observed as a loss of the fluorescent signal from the vesicle in response to a physiologically relevant 10 Hz train of stimulating electrical pulses (Figure 4B).

Aravanis et al.[106,107] found that upon stimulation, 85% of the fusing vesicles lost a subquantal portion of their fluorescence signal in a single fusion event (Figure 4B, 1), while a minority of 15% lost their entire fluorescence signal in a single event (Figure 4B, 2). Analysis of dwell times between initial stimulation and 20% fluorescence loss indicated that the majority of observed fusion events arose from vesicles in the readily releasable pool of vesicles. Further, the times over which fluorescence decreased from 20 to 80% indicated that the vesicles did not experience complete collapse during fusion. By unambiguously following the behavior of individual particles, they observed single vesicles undergoing multiple kiss-and-run fusion events (Figure 4B, 1). The latency periods (i.e., number of stimuli) for the first and second fusion events were ∼5 and ∼7 stimulating electrical pulses, respectively. Thus, it appeared that a vesicle could undergo repeated fusion events following a rapid retrieval or "re-priming" event, which retained large amounts of vesicular contents and caused the latency of a second fusion event to be slightly longer than that of the first.

Slow, subquantal fluorescence loss was confirmed by Richards et al.[19] using a similar experimental design, but with an elevated potassium concentration as a stimulus. Their calculations estimated that the kiss-and-run fusion pore had an ∼1 nm diameter. While transient, these noncomplete fusion events still give rise to lipid mixing between the vesicle and the plasma membrane.[20] Subquantal content loss is stimulation-dependent, however, and either disappears or cannot be resolved via high-frequency stimulation at 100 Hz, where only full quantal release was observed.[110]

Zhang et al.[109] incorporated bright quantum dots (Qdot) to label hippocampal synaptic vesicles and directly detected both kiss-and-run and complete fusion. In contrast to the loss of the

FM1−43 fluorescence signal, the Qdot emission intensity increased ∼15% upon opening of a kiss-and-run fusion pore, because of neutralization of the acidic intravesicular pH upon pore opening. This persistent fluorescence signal allowed Zhang et al. to resolve multiple kiss-and-run fusion events in single vesicles with improved signal-to-noise ratios and extended observation times. Kiss-and-run events were easily distinguished from complete fusion events, which were observed as a full loss of fluorescent signal and subsequent diffusion of the Qdot from a fusion site. They found that, initially, kiss-and-run fusion was the predominant type of fusion and arose from the readily releasable pool of vesicles but that complete fusion became dominant after extended stimulation. Kinetically, kiss-and-run fusion events had shorter latencies than complete fusion at stimulation frequencies of 0.1 and 10 Hz, though vesicles exhibiting kiss-and-run fusion would eventually undergo complete fusion. For the vesicles exhibiting kiss-and-run fusion, those undergoing the largest number of kiss-and-run events prior to complete fusion displayed the shortest latency period between subsequent events. Together, the observations of Zhang et al. indicate that the readily releasable pool of vesicles favors kiss-and-run fusion that have shorter latency periods. Once these vesicles are depleted and replenished by vesicles from a reserve pool, the likelihood of a kiss-and-run event diminishes and the full fusion events displaying a longer latency become predominant.

A recent study measured a lower bound on the number of SNARE complexes required for exocytotic fusion in vivo. Sinha et al.[111] fused the specialized pH-sensitive fluorescent protein pHluorin[25] to the luminal portion of the v-SNARE Syb2 protein. These pHl−Syb2 proteins were readily incorporated into hippocampal neuron synaptic vesicles. Initially, the fluorescence of the pHluorin was quenched within the acidic synaptic vesicle, but stimulation-induced fusion caused a quantal fluorescence increase upon neutralization of the acidic lumen. Plotting the distributions of fluorescence increases showed several equally spaced peaks, and photobleaching analysis indicated that each peak corresponded to a single pHl−Syb2 protein within the synaptic vesicles. Measurements made with neuronal cells containing only pHl-labeled Syb2 proteins resulted in a multipeak distribution lacking a peak at one quantum, whereas neurons having both labeled and unlabeled Syb2 gave a distribution with a distinct one-quantum peak. Sinha et al. thus concluded that a minimal fusion SNARE complex required two Syb2 proteins. Because each assembled SNARE complex is estimated to have ∼35 k_BT (21 kcal/mol)[112] of energy available, the coordinated effect of two Syb2 proteins would be more than sufficient to surmount the initial energy barrier separating the initial barriers to fusion (see the introductory section).

Taken together, these studies of SNARE-mediated fusion have identified at least two regimes of fusion kinetics that are found in vivo and two regimes in vitro. The in vivo situation appears to be linked to a shift from vesicles initially present at the membrane to the recruitment of vesicles from the cellular interior, transitioning from shorter latency periods to longer ones. The in vitro regimes are likely tied to the dependencies of the SNARE process on accessory proteins. These results hint at regulatory processes that control these fusion machines to appropriately enhance their fusogenicity or to restrict their catalytic potential, i.e., full vesicular membrane merger, and allow only partial content release.

OUTLOOK

The experimental approaches described here provide a solid foundation for moving forward on a number of fronts. With respect to further investigations into general aspects of membrane fusion, lipid dependencies for the various fusion systems can be probed in a straightforward manner. Target bilayers studied in in vitro systems can be readily manipulated to incorporate a range of lipid types, and these lipids can be exogenously added and incorporated into in vivo systems. Lipids such as lysophosphatidylcholine are considered to inhibit HA-mediated cell−cell fusion through a change in membrane curvature.[113] Demonstration of this effect in single-particle fusion assays of both HA fusion and SNARE fusion would establish the role of curvature as a general property affecting protein-mediated fusion as catalyzed by the fully intact systems. Cholesterol is another molecular player whose role in fusion has not been fully clarified, being required for some viruses to fuse and irrelevant for others. Single-particle assays could potentially distinguish if an effect of cholesterol arises from requirements regarding lipid arrangements or if the effect arises at the level of interactions between the fusion protein and proximal lipid components. With respect to experimental advances, the differentiation of distal leaflet mixing from proximal leaflet mixing at the single-particle level would provide another level of understanding regarding expansion of a lipidic fusion pore.

With regard to fusion-specific scenarios, mutational studies in conjunction with single-particle fusion detection can firmly establish the role of environmental sensitivities and of critical amino acid residues in governing fusion behavior. Relatedly, live-cell single-particle fusion studies can aid in delineating the role that additional cellular factors play in modulating fusion mechanisms. SNARE-related fusion relies on intracellular transport and signaling pathways to shift appropriately between the readily releasable pool and reserve pool of fusion vesicles. Viral fusion, too, can require dynamic cellular components, for instance, the molecular trigger causing pH-independent HIV-1 Env-mediated content release within an endosome that is not present at the cellular surface.

Technical advances can also play a role, most predominantly in the area of automated data selection. All single-particle studies require, first, experimental optimization to obtain high signal-to-noise ratios in the recorded fusion movies. Once this initial step is achieved, an equally difficult challenge is presented in the extraction and analysis of the fluorescence time trajectories. These challenges can require extensive computer programming, frequently supplemented by manual selection of fusion events, an analysis strategy that can take days to weeks once a successful experimental run is obtained.[81,94] While the development of automated analysis algorithms is time-consuming, the result can decrease analysis time up to 100-fold.[114] Some steps toward this automatization have been taken with live-cell studies of exocytosis and are reviewed briefly by Burchfield et al.[115] Similarities in the fluorescence signal obtained for both in vitro and in vivo studies of viral and SNARE fusion (Figure 2, and compare Figures 3 and 4) could allow for unification of analysis strategies among the diverse areas of study and contributing research groups. Progress on this front, in particular, has the potential to drive the field forward by facilitating many more experimental permutations to be performed within a single study, provided by less time-consuming and more consistent data analysis.

AUTHOR INFORMATION

Corresponding Author

*E-mail: a.m.van.oijen@rug.nl. Telephone: +31-50-363-9883. Fax: +31-50-363-9199.

Funding

A.M.v.O. would like to thank the Netherlands Organization for Scientific Research (NWO) and the European Research Council for support. J.O. would like to thank the National Institutes of Health (NIH) and the National Institute of General Medical Sciences (NIGMS) for the Molecular Biophysics Training Grant.

Notes

The authors declare no competing financial interest.

ABBREVIATIONS

Qdot, quantum dot; SLB, supported lipid bilayer; SNAP25, synaptosomal-associated protein 25; Syb, synaptobrevin-2; Syt, synaptotagmin-1; Syx, syntaxin-1; TIRFM, total internal reflection fluorescence microscopy.

REFERENCES

(1) Chernomordik, L. V., and Kozlov, M. M. (2003) Protein-lipid interplay in fusion and fission of biological membranes. *Annu. Rev. Biochem. 72*, 175−207.

(2) Markvoort, A. J., and Marrink, S. J. (2011) Lipid acrobatics in the membrane fusion arena. *Curr. Top. Membr. 68*, 259−294.

(3) Efrat, A., Chernomordik, L. V., and Kozlov, M. M. (2007) Point-like protrusion as a prestalk intermediate in membrane fusion pathway. *Biophys. J. 92*, L61−L63.

(4) Kuzmin, P. I., Zimmerberg, J., Chizmadzhev, Y. A., and Cohen, F. S. (2001) A quantitative model for membrane fusion based on low-energy intermediates. *Proc. Natl. Acad. Sci. U.S.A. 98*, 7235−7240.

(5) Jackson, M. B. (2011) Inferring structures of kinetic intermediates in Ca^{2+}-triggered exocytosis. *Curr. Top. Membr. 68*, 185−208.

(6) Melikyan, G. B., White, J. M., and Cohen, F. S. (1995) GPI-anchored influenza hemagglutinin induces hemifusion to both red blood cell and planar bilayer membranes. *J. Cell Biol. 131*, 679−691.

(7) Chernomordik, L. V., and Kozlov, M. M. (2005) Membrane hemifusion: Crossing a chasm in two leaps. *Cell 123*, 375−382.

(8) Niles, W. D., and Cohen, F. S. (1991) Fusion of influenza virions with a planar lipid membrane detected by video fluorescence microscopy. *J. Gen. Physiol. 97*, 1101−1119.

(9) Blumenthal, R., Gallo, S. A., Viard, M., Raviv, Y., and Puri, A. (2002) Fluorescent lipid probes in the study of viral membrane fusion. *Chem. Phys. Lipids 116*, 39−55.

(10) Wang, T., Smith, E. A., Chapman, E. R., and Weisshaar, J. C. (2009) Lipid mixing and content release in single-vesicle, SNARE-driven fusion assay with 1−5 ms resolution. *Biophys. J. 96*, 4122−4131.

(11) Kyoung, M., Srivastava, A., Zhang, Y., Diao, J., Vrljic, M., Grob, P., Nogales, E., Chu, S., and Brunger, A. T. (2011) In vitro system capable of differentiating fast Ca^{2+}-triggered content mixing from lipid exchange for mechanistic studies of neurotransmitter release. *Proc. Natl. Acad. Sci. U.S.A. 108*, 11737−11738.

(12) Diao, J., Grob, P., Cipriano, D. J., Kyoung, M., Zhang, Y., Shah, S., Nguyen, A., Padolina, M., Srivastava, A., Vrljic, M., Shah, A., Nogales, E., Chu, S., and Brunger, A. T. (2012) Synaptic proteins promote calcium-triggered fast transition from point contact to full fusion. *elife 1*, e00109.

(13) Wombacher, R., and Cornish, V. W. (2011) Chemical tags: Applications in live cell fluorescence imaging. *J. Biophotonics 4*, 391−402.

(14) Dieterich, D. C. (2010) Chemical reporters for the illumination of protein and cell dynamics. *Curr. Opin. Neurobiol. 20*, 623−630.

(15) Reymond, L., Lukinavicius, G., Umezawa, K., Maurel, D., Brun, M. A., Masharina, A., Bojkowska, K., Mollwitz, B., Schena, A., Griss, R., and Johnsson, K. (2011) Visualizing biochemical activities in living cells through chemistry. *Chimia (Aarau) 65*, 868−871.

(16) Cairo, C. W., Key, J. A., and Sadek, C. M. (2010) Fluorescent small-molecule probes of biochemistry at the plasma membrane. *Curr. Opin. Chem. Biol. 14*, 57−63.

(17) Yano, Y., and Matsuzaki, K. (2009) Tag-probe labeling methods for live-cell imaging of membrane proteins. *Biochim. Biophys. Acta 1788*, 2124−2131.

(18) Bissig, C., Johnson, S., and Gruenberg, J. (2012) Studying lipids involved in the endosomal pathway. *Methods Cell Biol. 108*, 19−46.

(19) Richards, D. A., Bai, J., and Chapman, E. R. (2005) Two modes of exocytosis at hippocampal synapses revealed by rate of FM1−43 efflux from individual vesicles. *J. Cell Biol. 168*, 929−939.

(20) Taraska, J. W., and Almers, W. (2004) Bilayers merge even when exocytosis is transient. *Proc. Natl. Acad. Sci. U.S.A. 101*, 8780−8785.

(21) Chudakov, D. M., Matz, M. V., Lukyanov, S., and Lukyanov, K. A. (2010) Fluorescent proteins and their applications in imaging living cells and tissues. *Physiol. Rev. 90*, 1103−1163.

(22) Day, R. N., and Davidson, M. W. (2009) The fluorescent protein palette: Tools for cellular imaging. *Chem. Soc. Rev. 38*, 2887−2921.

(23) Wiedenmann, J., Oswald, F., and Nienhaus, G. U. (2009) Fluorescent proteins for live cell imaging: Opportunities, limitations, and challenges. *IUBMB Life 61*, 1029−1042.

(24) Shaner, N. C., Steinbach, P. A., and Tsien, R. Y. (2005) A guide to choosing fluorescent proteins. *Nat. Methods 2*, 905−909.

(25) Miesenböck, G., De Angelis, D. A., and Rothman, J. E. (1998) Visualizing secretion and synaptic transmission with pH-sensitive green fluorescent proteins. *Nature 394*, 192−195.

(26) Fish, K. N. (2009) Total internal reflection fluorescence (TIRF) microscopy. *Current Protocols in Cytometry*, Chapter 12, Unit 12.18, Wiley, New York.

(27) Mattheyses, A. L., Simon, S. M., and Rappoport, J. Z. (2010) Imaging with total internal reflection fluorescence microscopy for the cell biologist. *J. Cell Sci. 123*, 3621−3628.

(28) Millis, B. A. (2012) Evanescent-wave field imaging: An introduction to total internal reflection fluorescence microscopy. *Methods Mol. Biol. 823*, 295−309.

(29) Yildiz, A., Forkey, J. N., McKinney, S. A., Ha, T., Goldman, Y. E., and Selvin, P. R. (2003) Myosin V walks hand-over-hand: Single fluorophore imaging with 1.5-nm localization. *Science 300*, 2061−2065.

(30) Manley, S., Gunzenhauser, J., and Olivier, N. (2011) A starter kit for point-localization super-resolution imaging. *Curr. Opin. Chem. Biol. 15*, 813−821.

(31) Czolkos, I., Jesorka, A., and Orwar, O. (2011) Molecular phospholipid films on solid supports. *Soft Matter 7*, 4562−4576.

(32) Richter, R. P., Berat, R., and Brisson, A. R. (2006) Formation of solid-supported lipid bilayers: An integrated view. *Langmuir 22*, 3497−3505.

(33) Nollert, P., Kiefer, H., and Jahnig, F. (1995) Lipid vesicle adsorption versus formation of planar bilayers on solid surfaces. *Biophys. J. 69*, 1447−1455.

(34) Brian, A. A., and McConnell, H. M. (1984) Allogeneic stimulation of cytotoxic T cells by supported planar membranes. *Proc. Natl. Acad. Sci. U.S.A. 81*, 6159−6163.

(35) Wagner, M. L., and Tamm, L. K. (2000) Tethered polymer-supported planar lipid bilayers for reconstitution of integral membrane proteins: Silane-polyethyleneglycol-lipid as a cushion and covalent linker. *Biophys. J. 79*, 1400−1414.

(36) Roder, F., Waichman, S., Paterok, D., Schubert, R., Richter, C., Liedberg, B., and Piehler, J. (2011) Reconstitution of membrane proteins into polymer-supported membranes for probing diffusion and interactions by single molecule techniques. *Anal. Chem. 83*, 6792−6799.

(37) Rawle, R. J., van Lengerich, B., Chung, M., Bendix, P. M., and Boxer, S. G. (2011) Vesicle fusion observed by content transfer across a tethered lipid bilayer. *Biophys. J. 101*, L37−L39.

(38) Floyd, D. L., Ragains, J. R., Skehel, J. J., Harrison, S. C., and van Oijen, A. M. (2008) Single-particle kinetics of influenza virus membrane fusion. *Proc. Natl. Acad. Sci. U.S.A. 105*, 15382−15387.
(39) Elender, G., Kuhner, M., and Sackmann, E. (1996) Functionalisation of Si/SiO_2 and glass surfaces with ultrathin dextran films and deposition of lipid bilayers. *Biosens. Bioelectron. 11*, 565−577.
(40) Skehel, J. J., Cross, K., Steinhauer, D., and Wiley, D. C. (2001) Influenza fusion peptides. *Biochem. Soc. Trans. 29*, 623−626.
(41) Harrison, S. C. (2005) Mechanism of membrane fusion by viral envelope proteins. *Adv. Virus Res. 64*, 231−261.
(42) Harrison, S. C. (2008) Viral membrane fusion. *Nat. Struct. Mol. Biol. 15*, 690−698.
(43) White, J. M., Delos, S. E., Brecher, M., and Schornberg, K. (2008) Structures and mechanisms of viral membrane fusion proteins: Multiple variations on a common theme. *Crit. Rev. Biochem. Mol. Biol. 43*, 189−219.
(44) Georgiou, G. N., Morrison, I. E., and Cherry, R. J. (1989) Digital fluorescence imaging of fusion of influenza virus with erythrocytes. *FEBS Lett. 250*, 487−492.
(45) Lowy, R. J., Sarkar, D. P., Chen, Y., and Blumenthal, R. (1990) Observation of single influenza virus-cell fusion and measurement by fluorescence video microscopy. *Proc. Natl. Acad. Sci. U.S.A. 87*, 1850−1854.
(46) Niles, W. D., and Cohen, F. S. (1991) The role of N-acetylneuraminic (sialic) acid in the pH dependence of influenza virion fusion with planar phospholipid membranes. *J. Gen. Physiol. 97*, 1121−1140.
(47) Wessels, L., Elting, M. W., Scimeca, D., and Weninger, K. (2007) Rapid membrane fusion of individual virus particles with supported lipid bilayers. *Biophys. J. 93*, 526−538.
(48) Ivanovic, T., Rozendaal, R., Floyd, D. L., Popovic, M., van Oijen, A. M., and Harrison, S. C. (2012) Kinetics of proton transport into influenza virions by the viral M2 channel. *PLoS One 7*, e31566.
(49) Imai, M., Mizuno, T., and Kawasaki, K. (2006) Membrane fusion by single influenza hemagglutinin trimers. Kinetic evidence from image analysis of hemagglutinin-reconstituted vesicles. *J. Biol. Chem. 281*, 12729−12735.
(50) Hoekstra, D., de Boer, T., Klappe, K., and Wilschut, J. (1984) Fluorescence method for measuring the kinetics of fusion between biological membranes. *Biochemistry 23*, 5675−5681.
(51) Loparo, J. J., and van Oijen, A. M. (2009) Single-Molecule Enzymology. In *Handbook of Single-Molecule Biophysics* (Hinterdorfer, P., and van Oijen, A., Eds.) 1st ed., pp 165−182, Springer, New York.
(52) Floyd, D. L., Harrison, S. C., and van Oijen, A. M. (2010) Analysis of kinetic intermediates in single-particle dwell-time distributions. *Biophys. J. 99*, 360−366.
(53) Bentz, J. (2000) Minimal aggregate size and minimal fusion unit for the first fusion pore of influenza hemagglutinin-mediated membrane fusion. *Biophys. J. 78*, 227−245.
(54) Melikyan, G. B., Niles, W. D., and Cohen, F. S. (1995) The fusion kinetics of influenza hemagglutinin expressing cells to planar bilayer membranes is affected by HA density and host cell surface. *J. Gen. Physiol. 106*, 783−802.
(55) Domanska, M. K., Kiessling, V., Stein, A., Fasshauer, D., and Tamm, L. K. (2009) Single vesicle millisecond fusion kinetics reveals number of SNARE complexes optimal for fast SNARE-mediated membrane fusion. *J. Biol. Chem. 284*, 32158−32166.
(56) Kiessling, V., Domanska, M. K., and Tamm, L. K. (2010) Single SNARE-mediated vesicle fusion observed in vitro by polarized TIRFM. *Biophys. J. 99*, 4047−4055.
(57) Liu, T., Wang, T., Chapman, E. R., and Weisshaar, J. C. (2008) Productive hemifusion intermediates in fast vesicle fusion driven by neuronal SNAREs. *Biophys. J. 94*, 1303−1314.
(58) Liu, T., Tucker, W. C., Bhalla, A., Chapman, E. R., and Weisshaar, J. C. (2005) SNARE-driven, 25-ms vesicle fusion in vitro. *Biophys. J. 89*, 2458−2472.
(59) Dobay, M. P., Dobay, A., Bantang, J., and Mendoza, E. (2011) How many trimers? Modeling influenza virus fusion yields a minimum aggregate size of six trimers, three of which are fusogenic. *Mol. BioSyst. 7*, 2741−2749.
(60) Huang, Q., Sivaramakrishna, R. P., Ludwig, K., Korte, T., Bottcher, C., and Herrmann, A. (2003) Early steps of the conformational change of influenza virus hemagglutinin to a fusion active state: Stability and energetics of the hemagglutinin. *Biochim. Biophys. Acta 1614*, 3−13.
(61) Lakadamyali, M., Rust, M. J., Babcock, H. P., and Zhuang, X. (2003) Visualizing infection of individual influenza viruses. *Proc. Natl. Acad. Sci. U.S.A. 100*, 9280−9285.
(62) Rust, M. J., Lakadamyali, M., Zhang, F., and Zhuang, X. (2004) Assembly of endocytic machinery around individual influenza viruses during viral entry. *Nat. Struct. Mol. Biol. 11*, 567−573.
(63) van der Schaar, H. M., Rust, M. J., Waarts, B. L., van der Ende-Metselaar, H., Kuhn, R. J., Wilschut, J., Zhuang, X., and Smit, J. M. (2007) Characterization of the early events in dengue virus cell entry by biochemical assays and single-virus tracking. *J. Virol. 81*, 12019−12028.
(64) Miyauchi, K., Kim, Y., Latinovic, O., Morozov, V., and Melikyan, G. B. (2009) HIV enters cells via endocytosis and dynamin-dependent fusion with endosomes. *Cell 137*, 433−444.
(65) Melikyan, G. B., Barnard, R. J. O., Abrahamyan, L. G., Mothes, W., and Young, J. A. T. (2005) Imaging individual retroviral fusion events: From hemifusion to pore formation and growth. *Proc. Natl. Acad. Sci. U.S.A. 102*, 8728−8733.
(66) Jha, N. K., Latinovic, O., Martin, E., Novitskiy, G., Marin, M., Miyauchi, K., Naughton, J., Young, J. A., and Melikyan, G. B. (2011) Imaging single retrovirus entry through alternative receptor isoforms and intermediates of virus-endosome fusion. *PLoS Pathog. 7*, e1001260.
(67) Markosyan, R. M., Cohen, F. S., and Melikyan, G. B. (2005) Time-resolved imaging of HIV-1 env-mediated lipid and content mixing between a single virion and cell membrane. *Mol. Biol. Cell 16*, 5502−5513.
(68) Padilla-Parra, S., Matos, P. M., Kondo, N., Marin, M., Santos, N. C., and Melikyan, G. B. (2012) Quantitative imaging of endosome acidification and single retrovirus fusion with distinct pools of early endosomes. *Proc. Natl. Acad. Sci. U.S.A. 109*, 17627−17632.
(69) Padilla-Parra, S., Marin, M., Kondo, N., and Melikyan, G. B. (2012) Synchronized retrovirus fusion in cells expressing alternative receptor isoforms releases the viral core into distinct sub-cellular compartments. *PLoS Pathog. 8*, e1002694.
(70) Brandenburg, B., and Zhuang, X. (2007) Virus trafficking: Learning from single-virus tracking. *Nat. Rev. Microbiol. 5*, 197−208.
(71) van der Schaar, H. M., Rust, M. J., Chen, C., van der Ende-Metselaar, H., Wilschut, J., Zhuang, X., and Smit, J. M. (2008) Dissecting the cell entry pathway of dengue virus by single-particle tracking in living cells. *PLoS Pathog. 4*, e1000244.
(72) de la Vega, M., Marin, M., Kondo, N., Miyauchi, K., Kim, Y., Epand, R. F., Epand, R. M., and Melikyan, G. B. (2011) Inhibition of HIV-1 endocytosis allows lipid mixing at the plasma membrane, but not complete fusion. *Retrovirology 8*, 99.
(73) Brunger, A. T., Weninger, K., Bowen, M., and Chu, S. (2009) Single-molecule studies of the neuronal SNARE fusion machinery. *Annu. Rev. Biochem. 78*, 903−928.
(74) Brunger, A. T. (2005) Structure and function of SNARE and SNARE-interacting proteins. *Q. Rev. Biophys. 38*, 1−47.
(75) Ma, C., Li, W., Xu, Y., and Rizo, J. (2011) Munc13 mediates the transition from the closed syntaxin-Munc18 complex to the SNARE complex. *Nat. Struct. Mol. Biol. 18*, 542−549.
(76) Llinas, R., Steinberg, I. Z., and Walton, K. (1981) Relationship between presynaptic calcium current and postsynaptic potential in squid giant synapse. *Biophys. J. 33*, 323−351.
(77) Heuser, J. (1989) The role of coated vesicles in recycling of synaptic vesicle membrane. *Cell Biol. Int. Rep. 13*, 1063−1076.
(78) Ceccarelli, B., Hurlbut, W. P., and Mauro, A. (1973) Turnover of transmitter and synaptic vesicles at the frog neuromuscular junction. *J. Cell Biol. 57*, 499−524.

(79) Kyoung, M., Zhang, Y., Diao, J., Chu, S., and Brunger, A. T. (2012) Studying calcium-triggered vesicle fusion in a single vesicle-vesicle content and lipid-mixing system. *Nat. Protoc. 8*, 1−16.
(80) Fix, M., Melia, T. J., Jaiswal, J. K., Rappoport, J. Z., You, D., Sollner, T. H., Rothman, J. E., and Simon, S. M. (2004) Imaging single membrane fusion events mediated by SNARE proteins. *Proc. Natl. Acad. Sci. U.S.A. 101*, 7311−7316.
(81) Karatekin, E., and Rothman, J. E. (2012) Fusion of single proteoliposomes with planar, cushioned bilayers in microfluidic flow cells. *Nat. Protoc. 7*, 903−920.
(82) Domanska, M. K., Kiessling, V., and Tamm, L. K. (2010) Docking and fast fusion of synaptobrevin vesicles depends on the lipid compositions of the vesicle and the acceptor SNARE complex-containing target membrane. *Biophys. J. 99*, 2936−2946.
(83) Karatekin, E., Di Giovanni, J., Iborra, C., Coleman, J., O'Shaughnessy, B., Seagar, M., and Rothman, J. E. (2010) A fast, single-vesicle fusion assay mimics physiological SNARE requirements. *Proc. Natl. Acad. Sci. U.S.A. 107*, 3517−3521.
(84) Yoon, T. Y., Okumus, B., Zhang, F., Shin, Y. K., and Ha, T. (2006) Multiple intermediates in SNARE-induced membrane fusion. *Proc. Natl. Acad. Sci. U.S.A. 103*, 19731−19736.
(85) Yoon, T. Y., Lu, X., Diao, J., Lee, S. M., Ha, T., and Shin, Y. K. (2008) Complexin and Ca^{2+} stimulate SNARE-mediated membrane fusion. *Nat. Struct. Mol. Biol. 15*, 707−713.
(86) Lee, H. K., Yang, Y., Su, Z., Hyeon, C., Lee, T. S., Lee, H. W., Kweon, D. H., Shin, Y. K., and Yoon, T. Y. (2010) Dynamic Ca^{2+}-dependent stimulation of vesicle fusion by membrane-anchored synaptotagmin 1. *Science 328*, 760−763.
(87) Smith, E. A., and Weisshaar, J. C. (2011) Docking, not fusion, as the rate-limiting step in a SNARE-driven vesicle fusion assay. *Biophys. J. 100*, 2141−2150.
(88) Bowen, M. E., Weninger, K., Brunger, A. T., and Chu, S. (2004) Single molecule observation of liposome-bilayer fusion thermally induced by soluble N-ethyl maleimide sensitive-factor attachment protein receptors (SNAREs). *Biophys. J. 87*, 3569−3584.
(89) Montecucco, C., Schiavo, G., and Pantano, S. (2005) SNARE complexes and neuroexocytosis: How many, how close? *Trends Biochem. Sci. 30*, 367−372.
(90) van den Bogaart, G., Holt, M. G., Bunt, G., Riedel, D., Wouters, F. S., and Jahn, R. (2010) One SNARE complex is sufficient for membrane fusion. *Nat. Struct. Mol. Biol. 17*, 358−364.
(91) Diao, J., Su, Z., Ishitsuka, Y., Lu, B., Lee, K. S., Lai, Y., Shin, Y. K., and Ha, T. (2010) A single-vesicle content mixing assay for SNARE-mediated membrane fusion. *Nat. Commun. 1*, 54.
(92) Christensen, S. M., Mortensen, M. W., and Stamou, D. G. (2011) Single vesicle assaying of SNARE-synaptotagmin-driven fusion reveals fast and slow modes of both docking and fusion and intrasample heterogeneity. *Biophys. J. 100*, 957−967.
(93) Lai, Y., Diao, J., Liu, Y., Ishitsuka, Y., Su, Z., Schulten, K., Ha, T., and Shin, Y. K. (2013) Fusion pore formation and expansion induced by Ca^{2+} and synaptotagmin 1. *Proc. Natl. Acad. Sci. U.S.A. 110*, 1333−1338.
(94) Diao, J., Ishitsuka, Y., Lee, H., Joo, C., Su, Z., Syed, S., Shin, Y. K., Yoon, T. Y., and Ha, T. (2012) A single vesicle-vesicle fusion assay for in vitro studies of SNAREs and accessory proteins. *Nat. Protoc. 7*, 921−934.
(95) Ge, S., Koseoglu, S., and Haynes, C. L. (2010) Bioanalytical tools for single-cell study of exocytosis. *Anal. Bioanal. Chem. 397*, 3281−3304.
(96) Keighron, J. D., Ewing, A. G., and Cans, A. S. (2012) Analytical tools to monitor exocytosis: A focus on new fluorescent probes and methods. *Analyst 137*, 1755−1763.
(97) Gandhi, S. P., and Stevens, C. F. (2003) Three modes of synaptic vesicular recycling revealed by single-vesicle imaging. *Nature 423*, 607−613.
(98) Balaji, J., and Ryan, T. A. (2007) Single-vesicle imaging reveals that synaptic vesicle exocytosis and endocytosis are coupled by a single stochastic mode. *Proc. Natl. Acad. Sci. U.S.A. 104*, 20576−20581.
(99) Aoki, R., Kitaguchi, T., Oya, M., Yanagihara, Y., Sato, M., Miyawaki, A., and Tsuboi, T. (2010) Duration of fusion pore opening and the amount of hormone released are regulated by myosin II during kiss-and-run exocytosis. *Biochem. J. 429*, 497−504.
(100) Bai, L., Wang, Y., Fan, J., Chen, Y., Ji, W., Qu, A., Xu, P., James, D. E., and Xu, T. (2007) Dissecting multiple steps of GLUT4 trafficking and identifying the sites of insulin action. *Cell Metab. 5*, 47−57.
(101) Jiang, L., Fan, J., Bai, L., Wang, Y., Chen, Y., Yang, L., Chen, L., and Xu, T. (2008) Direct quantification of fusion rate reveals a distal role for AS160 in insulin-stimulated fusion of GLUT4 storage vesicles. *J. Biol. Chem. 283*, 8508−8516.
(102) Jaiswal, J. K., Rivera, V. M., and Simon, S. M. (2009) Exocytosis of post-Golgi vesicles is regulated by components of the endocytic machinery. *Cell 137*, 1308−1319.
(103) Allersma, M. W., Wang, L., Axelrod, D., and Holz, R. W. (2004) Visualization of regulated exocytosis with a granule-membrane probe using total internal reflection microscopy. *Mol. Biol. Cell 15*, 4658−4668.
(104) Murthy, V. N., and Stevens, C. F. (1999) Reversal of synaptic vesicle docking at central synapses. *Nat. Neurosci. 2*, 503−507.
(105) Pyle, J. L., Kavalali, E. T., Piedras-Renteria, E. S., and Tsien, R. W. (2000) Rapid reuse of readily releasable pool vesicles at hippocampal synapses. *Neuron 28*, 221−231.
(106) Aravanis, A. M., Pyle, J. L., and Tsien, R. W. (2003) Single synaptic vesicles fusing transiently and successively without loss of identity. *Nature 423*, 643−647.
(107) Aravanis, A. M., Pyle, J. L., Harata, N. C., and Tsien, R. W. (2003) Imaging single synaptic vesicles undergoing repeated fusion events: Kissing, running, and kissing again. *Neuropharmacology 45*, 797−813.
(108) Murthy, V. N., and Stevens, C. F. (1998) Synaptic vesicles retain their identity through the endocytic cycle. *Nature 392*, 497−501.
(109) Zhang, Q., Li, Y., and Tsien, R. W. (2009) The dynamic control of kiss-and-run and vesicular reuse probed with single nanoparticles. *Science 323*, 1448−1453.
(110) Chen, X., Barg, S., and Almers, W. (2008) Release of the styryl dyes from single synaptic vesicles in hippocampal neurons. *J. Neurosci. 28*, 1894−1903.
(111) Sinha, R., Ahmed, S., Jahn, R., and Klingauf, J. (2011) Two synaptobrevin molecules are sufficient for vesicle fusion in central nervous system synapses. *Proc. Natl. Acad. Sci. U.S.A. 108*, 14318−14323.
(112) Li, F., Pincet, F., Perez, E., Eng, W. S., Melia, T. J., Rothman, J. E., and Tareste, D. (2007) Energetics and dynamics of SNAREpin folding across lipid bilayers. *Nat. Struct. Mol. Biol. 14*, 890−896.
(113) Chernomordik, L. V., Leikina, E., Frolov, V., Bronk, P., and Zimmerberg, J. (1997) An early stage of membrane fusion mediated by the low pH conformation of influenza hemagglutinin depends upon membrane lipids. *J. Cell Biol. 136*, 81−93.
(114) Mittal, A., Leikina, E., Chernomordik, L. V., and Bentz, J. (2003) Kinetically differentiating influenza hemagglutinin fusion and hemifusion machines. *Biophys. J. 85*, 1713−1724.
(115) Burchfield, J. G., Lopez, J. A., Mele, K., Vallotton, P., and Hughes, W. E. (2010) Exocytotic vesicle behaviour assessed by total internal reflection fluorescence microscopy. *Traffic 11*, 429−439.

■ NOTE ADDED AFTER ASAP PUBLICATION

This manuscript was published ASAP on February 19, 2013 with an incorrect value reported in the Diao et al. study. The corrected version was reposted to the Web on February 26, 2013.